



Research Paper

Day-Night Oscillation of *Atrogin1* and Timing-Dependent Preventive Effect of Weight-Bearing on Muscle Atrophy



Shinya Aoyama^{a,b}, Shuichi Kojima^a, Keisuke Sasaki^a, Ryosuke Ishikawa^a, Mizuho Tanaka^a, Takeru Shimoda^a, Yuta Hattori^a, Natsumi Aoki^{a,b}, Kengo Takahashi^a, Rina Hirooka^a, Miku Takizawa^a, Atsushi Haraguchi^a, Shigenobu Shibata^{a,*}

^a Laboratory of Physiology and Pharmacology, School of Advanced Science and Engineering, Waseda University, Tokyo, Japan,

^b Organization for University Research Initiatives, Waseda University, Tokyo, Japan

ARTICLE INFO

Article history:

Received 15 March 2018

Received in revised form 9 October 2018

Accepted 24 October 2018

Available online 1 November 2018

Keywords:

Circadian rhythm

Chrono-exercise

Atrogin1

Hindlimb-unloading

Weight-bearing

ABSTRACT

Background: *Atrogin1*, which is one of the key genes for the promotion of muscle atrophy, exhibits day-night variation. However, its mechanism and the role of its day-night variation are largely unknown in a muscle atrophic context.

Methods: The mice were induced a muscle atrophy by hindlimb-unloading (HU). To examine a role of circadian clock, Wild-type (WT) and *Clock* mutant mice were used. To test the effects of a neuronal effects, an unilateral ablation of sciatic nerve was performed in HU mice. To test a timing-dependent effects of weight-bearing, mice were released from HU for 4 h in a day at early or late active phase (W-EAP and W-LAP groups, respectively).

Findings: We found that the day-night oscillation of *Atrogin1* expression was not observed in *Clock* mutant mice or in the sciatic denervated muscle. In addition, the therapeutic effects of weight-bearing were dependent on its timing with a better effect in the early active phase.

Interpretation: These findings suggest that the circadian clock controls the day-night oscillation of *Atrogin1* expression and the therapeutic effects of weight-bearing are dependent on its timing.

Fund: Council for Science, Technology, and Innovation, SIP, “Technologies for creating next-generation agriculture, forestry, and fisheries”.

© 2018 The Authors. Published by Elsevier B.V. This is an open access article under the CC BY-NC-ND license (<http://creativecommons.org/licenses/by-nc-nd/4.0/>).

1. Introduction

Various physiological events, including the sleep wake cycle, body temperature, and locomotor activity, exhibit circadian rhythms. These day-night fluctuations are driven by an internal circadian clock. A mammalian circadian clock is divided into two parts: the central clock in the suprachiasmatic nucleus (SCN) of the hypothalamus and peripheral clocks in peripheral tissues [1]. The central clock in the SCN has a role as a time keeper, and orchestrates and integrates the peripheral circadian clocks via neuronal and hormonal signals such as the sympathetic nervous system and glucocorticoid signaling [2,3]. Light is the major entraining factor for the SCN. Peripheral clocks are entrained not only by neuronal and hormonal signals via light-dependent regulation of the central clock in the SCN but also additionally by feeding and locomotor activity stimuli independent from the central clock in the SCN [4–6]. The molecular system of a mammalian circadian clock consists of a

transcriptional and translational negative feedback loop of core clock genes, which include *Brain and muscle ARNT-like 1 (Bmal1)*, *Circadian locomotor output cycles kaput (Clock)*, *Period1 (Per1)*, *Period2 (Per2)*, *Cryptochrome1 (Cry1)*, and *Cryptochrome2 (Cry2)* [7]. In brief, a heterodimer of BMAL1 and CLOCK acts as a transcriptional factor for *Pers* and *Crys* via binding to their E-box binding element. After their transcription and translation, PER1,2 and CRY1,2 inhibit the CLOCK and BMAL1-induced transcription of *Pers* and *Crys* and are degraded by ubiquitination systems.

Circadian transcriptomic studies have revealed that global rhythmic genes expression occurs in a tissue-specific manner, suggesting that the peripheral clocks generate the circadian fluctuation of tissue-specific physiological functions [8,9]. The circadian transcriptomes of mouse and human adult skeletal muscle have been reported [8,10–13], and the rhythmic gene expression is muscle-fiber type-specific [10]. In skeletal muscle, it is thought that the rhythm of muscular gene expression is regulated not only by an intrinsic muscle clock but additionally by feeding time and locomotor activity [10,14,15]. These rhythmic genes include several muscle-specific genes, such as *Myogenic differentiation*

* Corresponding author at: Wakamatsu-cho 2-2, Tokyo 162-8480, Japan.
E-mail address: shibatasa@waseda.jp (S. Shibata).

Research in context

Evidence before this study

Atrogin1 is a key regulator of catabolism in muscles and circadian transcriptome studies have revealed its rhythmic expression in adult healthy muscles. However, its rhythmic expression in the atrophic muscle and its contribution to muscle atrophy are yet unknown. We searched PubMed for transgenic mouse studies involving the clock genes and focused on muscle function, using “circadian rhythm” or “clock gene” and “skeletal muscle” as search terms. Some papers reviewed muscle dysfunction in clock gene transgenic mice. For example, whole-body *Bmal1* knockout mice exhibit muscle loss; however, muscle-specific knockout mice do not. In addition to data on transgenic mice, we searched for studies on the day-night variation of muscle catabolic processes. Such variation was assessed, to our knowledge, only in two atrophic models of fasting and denervation.

Added value of this study

A key insight obtained in this study is the importance of timing in preventive or therapeutic interventions against muscle loss based on exercise and rehabilitation.

Implications of all the available evidence

The day-night oscillations of *Atrogin1* expression shown in this study may provide a target for muscle chrono-therapy. Our findings underline the importance of circadian timing in designing exercise and rehabilitation interventions.

1 (*Myod1*), *Uncoupling protein 3* (*Ucp3*), *F-box protein 32* (*Atrogin1*), and *Myosin heavy chain 1* (*Myh1*), suggesting that the circadian clock regulates muscle functions. Indeed, mice with a clock gene deletion or mutation exhibit muscle dysfunctions such as an early age-related muscle loss, weak muscle strength, low oxidative capacity and glucose intolerance [11,16–22]. In contrast, muscle-specific *Bmal1* knockout mice did not exhibit muscle loss [11]. The regulation of muscle volume by the circadian clock has not been fully elucidated.

Muscle loss is observed in various physiological conditions and chronic diseases such as aging, malnutrition, bed rest, immobilization, neurodegeneration, muscle dystrophy, cancer cachexia, diabetes and sepsis. In general, muscle mass is controlled by a balance between muscle protein anabolic and catabolic processes. An excessive increase in protein degradation induces muscle atrophy, which has been observed in many muscle atrophic conditions [23]. Importantly, a remarkable increase in ubiquitin proteasome activity, one of the major protein catabolic processes, has been observed in atrophic muscles [24]. In 2001, two E3 ubiquitin ligases, *Atrogin1* and *Murf1*, were identified as trigger molecules for muscle atrophy progression [25,26]. These genes are increased in many muscle atrophy models, including disuse and a microgravity models [23], and the *Atrogin1* and *Murf1* knockout mice show attenuated denervation-induced muscle atrophy [25]. Importantly, these knockout mice exhibit normal growth and muscle phenotypes throughout development [23], suggesting the action of *Atrogin1* and *Murf1* is limited to a muscle atrophic condition. As described previously, *Atrogin1* and *Murf1* expressions exhibit a circadian rhythm in adult skeletal muscle, and *Atrogin1* expression is up-regulated in *Clock* mutant mice [12]. However, their rhythmic expressions and the role of the circadian clock have not been thoroughly investigated in atrophic conditions, with only a study of a denervation-induced muscle atrophy model being reported [27].

Physical inactivity and immobility induced muscle loss, and weight-bearing exercise is effective therapy for prevention of disused-muscle atrophy. An intermittent weight-bearing routine attenuates an increase of *Atrogin1* and *Murf1* expressions in the muscles of hindlimb unloaded (HU) mice [28,29]. However, a timing-dependent effect of weight-bearing has not yet been studied, although it has been suggested that muscle catabolic processes and muscle mass are controlled by a circadian clock [12,18].

In the present study, we examined the expression rhythm of *Atrogin1* and *Murf1* under the HU condition and the role of the circadian clock on their expression rhythm and muscle loss. Additionally, we investigate a timing-dependent preventive effect of intermittent weight-bearing on a HU-induced muscle atrophy.

2. Materials and methods

2.1. Animals

Six-week-old male Kwi:ICR mice (body weight: 25.7–34.8 g) were obtained from Tokyo Laboratory Animals Science. C57BL:6 *J-Clock^{mlJ}*:J (*Clock* mutant) mice were obtained from Jackson Laboratory (RRID: IMSR_JAX:002923) and backcrossed to ICR mice in our previous report [30]. Six- to ten-week-old male wild-type (WT; body weight: 27.6–42.7 g) and *Clock* mutant (*Clock^{Δ19}*; body weight: 27.7–42.0 g) mice backcrossed to ICR mice were used. The animal facility is operated as a conventional room. Mice were kept in a room maintained at 22 ± 2°C, 60 ± 5% humidity on a 12-h light (08:00–20:00)–dark cycle. Zeitgeber time 0 (ZT0) was designated as lights-on time and ZT12 as lights-off time. The mice were provided with a standard diet (EF; Oriental Yeast) and water ad libitum. All mice were in group housing (4 mice per cage) during the acclimation period, and subsequently singly housed during experimental periods. After randomized grouping, experiments were conducted in a nonblinded condition. This study was approved by the Committee for Animal Experimentation at Waseda University (2017-A070) and animals were treated in accordance with the committee's guidelines.

2.2. Hindlimb-unloading and weight-bearing

Hindlimb-unloading was performed as described previously [31]. A plastic band was fixed to the root and middle region of the mouse tail with surgical tape under isoflurane anesthesia. Three days after attachment of the plastic band, a rod was connected to the plastic band via a fishing swivel and the other end of the rod was attached to the top of the cage. Mice were able to move freely with their front legs and were allowed access to food and water without contact of each hindfoot to the floor. Intermittent weight-bearing was performed using a timing-regulated weight-bearing apparatus. Its design is shown in Supplementary Fig. 1. The intermittent weight-bearing was automatically regulated by a magnetic switch connected to a timer.

2.3. Ablation of the sciatic nerve

The unilateral sciatic nerve was excised as described previously [32]. Briefly, excision of the sciatic nerve was performed for the right leg, and sham surgery was performed for the left leg of each mouse during the same operation under isoflurane anesthesia (Wako Chemicals).

2.4. Measurement of locomotor activity

Locomotor activity of mice was monitored with an area sensor (F5B; Omron) and analyzed with ClockLab software (Actimetrics) as previously described [33]. Locomotor activity was continuously monitored during experimental periods.

2.5. Histological analysis

The gastrocnemius muscles were isolated for hematoxylin and eosin (H&E) staining. The muscles were frozen in a liquid nitrogen-cooled isopentane (Wako Chemicals). Subsequently, ten or sixteen-micrometer thick cross sections were cut from the middle portion of the muscle using a cryostat (Leica Microsystems). Sections were fixed in 10% formalin neutral buffer (Wako Chemicals) and then stained with hematoxylin solution (Wako Chemicals) followed by the eosin solution (Wako Chemicals). Cross-sectional area (CSA) of muscle fibers was determined using BZ-X analyzer software (Keyence). >500 fibers per mouse were analyzed from three areas in each muscle.

2.6. Measurement of serum corticosterone

Serum corticosterone levels were measured using a commercial kit (ASSAYPRO). Assays were performed according to the manufacturer's instructions.

2.7. Total RNA extraction and Real-time RT-PCR

Total RNA in skeletal muscle was extracted with TRIzol reagents (Thermo Fisher Scientific). Real-time reverse transcription PCR was performed using the One-Step SYBR RT-PCR Kit (Takara Bio Inc) with specific primer pairs (Supplementary Table 1) on a Piko Real PCR system (Thermo Fisher Scientific). The relative expression levels of target genes were normalized to those of *TATA box binding protein (Tbp)*. Data were analyzed using the $\Delta\Delta C_t$ method as described in our previously reports [33].

2.8. Protein extraction and western blotting

Frozen gastrocnemius muscles were ground into a powder using a frozen cell crusher (Cryo-Press, MICROTEC, Tokyo, Japan) and homogenized using Tissuelyser II (Qiagen, Frederick, MD, USA) with RIPA buffer (50 mM Tris-HCl pH 7.6, 150 mM NaCl, 1 mM EDTA, 1% TritonX-100, 1% sodium deoxycholate, 0.1% SDS) in the presence of protease inhibitor cocktail (Roche Diagnostics, Indianapolis, IN, USA), and phosphatase inhibitor cocktail (Nacalai Tesque, Kyoto, Japan). After homogenizing, samples were rotated for 1.5 h at 4 °C, then centrifuged at 14,000 ×g for 30 min at 4 °C. Protein concentrations were measured with a BCA protein assay kit (Thermo Fisher Scientific). Western blotting analysis was conducted as described previously [32]. SDS-PAGE was performed with 20 or 50 µg of protein and the proteins in the gel were transferred onto polyvinylidene difluoride (PVDF) membranes (GE Healthcare, Buckinghamshire, UK). The membranes were then incubated overnight at 4 °C with anti-p70S6K antibody (1:1000 dilution), anti-phospho-p70S6K antibody (1:1000 dilution), anti-phospho-S6 antibody (1:1000 dilution), anti-S6 antibody (1:1000 dilution), anti-phospho-Akt antibody (1:1000 dilution), anti-Akt antibody (1:1000 dilution) or anti-glyceraldehyde 3-phosphate dehydrogenase (GAPDH) antibody (1:250 dilution). Phospho-p70S6 kinase (Thr389) antibody (Cat#9205, RRID:AB_330944), p70S6 kinase antibody (Cat#9202, RRID:AB_331676), Phospho-S6 (Ser240, Ser244) antibody (Cat#2215, RRID:AB_331683), S6 antibody (Cat#2217, RRID:AB_331355), phospho-Akt (Ser473) antibody (Cat#9271, RRID:AB_329825), Akt-antibody (Cat#9272, RRID:AB_329827) and horseradish peroxidase (HRP)-conjugated anti-rabbit IgG antibody (Cat# 7074, RRID:AB_2099233) were purchased from Cell Signaling Technology (Danvers, MA, USA). Anti-GAPDH antibody (Cat# sc-20,357, RRID:AB_641107) and HRP-conjugated anti-goat IgG antibody (Cat# sc-2020, RRID:AB_631728) were purchased from SantaCruz biotechnology (Santa Cruz, CA, USA). The bands of immunoreactive proteins were detected with an enhanced chemiluminescence kit (GE Healthcare, Buckinghamshire, UK) and quantified using a LAS-3000 system (GE healthcare, Buckinghamshire, UK).

2.9. Statistical analysis

Data are represented as mean ± SE values. The GraphPad Prism version 7 (GraphPad Software) was used for the statistical analysis. $P < .05$ was considered as a statistically significant difference. To test whether data (sample size: $n > 4$) showed normal or non-normal distribution and equal or biased variation, we used Kolmogorov-Smirnov test and an *F*-test or Brown-Forsythe's test, respectively. If the data showed normal distribution and equal variation, statistical significance was determined by unpaired *t*-test or a one-way ANOVA with a Tukey test or two-way ANOVA with a Tukey test (if the interaction was significant) or Sidak test (if the interaction was not significant but the main effect was significant) for post-hoc analysis. If the data showed non-normal distribution or biased variation, statistical significance was determined by Mann-Whitney *U* test or Kruskal-Wallis test with a two-stage linear step-up procedure of the Benjamini, Krieger, and Yekutieli test for multiple comparisons. For the data of small sample size ($n < 5$), the statistical significance was determined using the Mann-Whitney *U* test or Kruskal-Wallis test with a two-stage linear step-up procedure of the Benjamini, Krieger, and Yekutieli test for multiple comparisons. Value of *n* in the figure legends represents the number of animals (The details were shown in Supplementary Table 2). The statistical details of experiments were shown in the figure legends and Supplementary Table 3. The JTK_cycle algorithm was used to detect 24-h rhythms and to analyze day-night variation and amplitude [34,35]. The results of the JTK cycle algorithm were listed in Supplementary Table 4.

3. Results

3.1. Day-night fluctuations of catabolic processes in HU-induced atrophic muscles

Mice were placed into the HU model for 3 to 4 days to test whether the *Atrogin1* and *Murf1* showed day-night variation in a muscle atrophy progressing condition (Fig. 1a). HU increased *Atrogin1* expression significantly in the gastrocnemius muscle, and the gene exhibited day-night variation, which was lower at ZT9 and higher at ZT21 (Fig. 1b and Supplementary Table 4). *Murf1* expression likewise exhibited day-night variation in a similar pattern as *Atrogin1*, though the level of *Murf1* was not increased by HU (Fig. 1c and Supplementary Table 4). The clock gene expressions including *Per1*, *Per2*, *Bmal1*, *Rev-erba*, and *Rora* showed circadian oscillation in the gastrocnemius muscle from CON and HU mice, and *Per1* and *Rora* expressions were increased by HU (Fig. 1d–h and Supplementary Table 3). The serum corticosterone level of HU group tended to be increased, and its circadian rhythm was maintained (Fig. 1f and Supplementary Table 4). Glucocorticoids receptor gene expression was not changed among all group and time points (Supplementary Fig. 2b). Phosphorylation of p70S6K, S6 and Akt, the key molecules for muscle anabolic processes, did not show day-night variation in both groups, and S6 and Akt phosphorylation were partially decreased by HU (Fig. 1k–m and Supplementary Tables 3 and 4). In the soleus muscle, *Atrogin1* and *Murf1* were increased by HU, however they were not changed over a day (Supplementary Fig. 3a and b). *Per2* and *Bmal1* showed circadian oscillation in the soleus muscle (Supplementary Fig. 3c and d and Supplementary Table 4). Furthermore, the peak time and periods of PER2::LUC luminescence in SCN slice were not changed among all groups (Supplementary Fig. 4).

3.2. Circadian clock drives HU-induced day-night expression of *Atrogin1* and *Murf1*

To confirm the role of a circadian clock on the day-night expressions of *Atrogin1* and *Murf1*, these expressions were assessed in the muscles of *Clock^{Δ19}* mice. In WT mice, *Atrogin1* expression was increased by HU for 3 to 4 days and it showed the day-night fluctuation, while its fluctuation was not observed in *Clock^{Δ19}* mice (Fig. 2a and

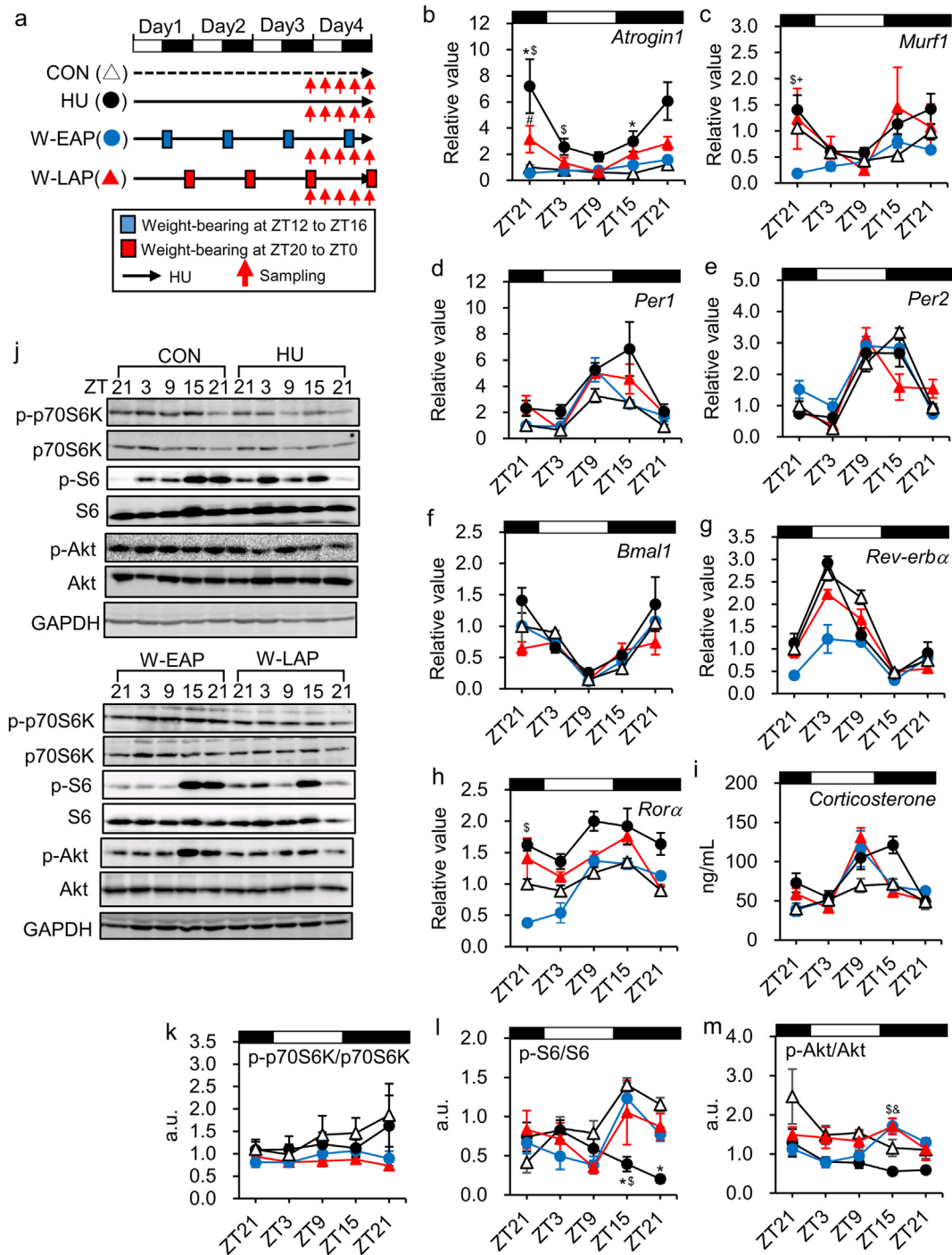


Fig. 1. Day-night variations of muscle catabolic gene, clock genes expressions, serum corticosterone level, and phosphorylation of muscle anabolic protein in Control (CON), Hindlimb unloading (HU) and weight-bearing during early (W-EAP) and late (W-LAP) active phase mice. (a) Experimental scheme for evaluating the day-night variations in the CON, HU, W-EAP and W-LAP mice. The mice in the HU group were kept in the HU condition for 3 or 4 days. The mice in the W-EAP and W-LAP group were kept under the HU condition except for the period of weight-bearing. Intermittent weight-bearing at the early and late active phases was conducted from ZT12 to ZT16 and from ZT20 to ZT24, respectively, as shown in blue and red square. The muscles were collected every 6 h from ZT21 on day 3 to ZT21 on day 4, as indicated by the red arrows. White and black bars indicate light (inactive) and dark (active) phase. The gene expression levels of (b) *Atrogin1*, (c) *Murf1*, (d) *Per1*, (e) *Per2*, (f) *Bmal1*, (g) *Rev-erba* and (h) *Rora* in gastrocnemius muscle of CON (white triangles), HU (black circles), W-EAP (blue circles) and W-LAP (red triangles) mice. (i) Serum corticosterone level was determined by ELISA. (j) Western blot analysis for the phosphorylation of p70S6K, S6 and Akt in gastrocnemius muscle. (k – m) Quantitative signal intensity ratio of phosphorylated p70S6K, S6 and Akt to total respective proteins. Data are expressed as the mean \pm standard error ($n = 4-5$ at each time point). * $P < .05$; CON vs HU, + $P < .05$; CON vs W-EAP, \$ $P < .05$; HU vs W-EAP, & $P < .05$; HU vs W-LAP, # $P < .05$; W-EAP vs W-LAP by Kruskal-Wallis test with a two-stage linear step-up procedure of Benjamini, Krieger and Yekutieli test.

Supplementary Table 4). *Murf1* expression in *Clock*^{Δ19} mice was partially increased by HU and its time-dependent expression was not observed (Fig. 2b and Supplementary Table 4). We next evaluated the muscle weight in the hindlimb-unloaded WT and *Clock*^{Δ19} mice. HU

for 2 weeks significantly decreased gastrocnemius muscle weight in the WT and *Clock*^{Δ19} mutant mice (Fig. 2c and d). The ratio of HU muscle weight to CON muscle in *Clock*^{Δ19} mice was significantly decreased compared with WT mice (Fig. 2e).

Considering that the expressions of *Atrogin1* and *Murf1* were regulated by nutritional statement via an insulin and IGFs signaling pathway [36] and the feeding behavior of mice showed a circadian manner, we next examined an effect of time-restricted feeding on the day-night expression of *Atrogin1* and *Murf1* to reveal a feeding cycle-dependent regulation of their rhythmic expressions. Mice were kept under the day-time (ZT2 to ZT10, DRF) or night-time (ZT14 to ZT22, NRF) restricted feeding schedule for 7 days before and 4 days after HU (Supplementary Fig. 5a). The day-night expressions of *Atrogin1* and *Murf1* were not changed between the DRF and NRF mice (Supplementary Fig. 5b and c), suggesting that the fluctuations of *Atrogin1* and *Murf1* expression could be independent of feeding time. In addition, the expression of clock genes except *Rorα*, which did not show circadian rhythmicity under the HU condition (Supplementary Table 4), exhibited an antiphase oscillation in the gastrocnemius muscle of day- and night-time-restricted feeding groups (Supplementary Fig. 5d–h). Moreover, the amplitude of *Bmal1* was decreased by DRF mice (Supplementary Table 4). This suggested that the day-night fluctuations of *Atrogin1* and *Murf1* were independent of the intrinsic muscle clock, and these fluctuations could be controlled by a time-dependent external signal such as neuronal and hormonal signals from the SCN.

Circadian oscillated genes in the skeletal muscle were regulated by the intrinsic muscle clock, locomotor activity, neuronal and hormonal stimulus, and feeding cycle [10,11,14]. We next determined the role of locomotor activity and neuronal signals on the day-night variation of *Atrogin1* in the HU condition using the combination of HU model and sciatic denervation model. Mice were subjected to the unilateral ablation of the sciatic nerve before the induction of HU (Fig. 3a). The day-night expression of *Atrogin1* was not observed in the denervated muscle of HU mice, while it was observed in the sham-surgery contralateral muscle of HU mice (Fig. 3b). HU and denervation increased *Atrogin1* level, and their combination further increased it. *Murf1* expression showed day-night fluctuation in the denervated muscle of CON mice (Fig. 3c). The denervation increased *Per2*, *Bmal1*, and *Rorα* expression and abolished the rhythmicity of *Rorα* (Fig. 3). The rhythmicity and

phase of clock genes expression except for *Rorα* remained in the denervated muscles (Fig. 3),

3.3. Timing-dependent effect of weight-bearing on HU-induced muscle atrophy

To assess the effective timing of a weight-bearing on *Atrogin1* and *Murf1* expressions, mice were intermittently relieved from HU at a specific time within a day (Supplementary Fig. 1) and skeletal muscles were collected at 5 points within 3 to 4 days (Fig. 1a). Weight-bearing at the early active phase (W-EAP) significantly suppressed *Atrogin1* and *Murf1* expressions at 1st ZT21, when *Atrogin1* was at a high point of its oscillation within a day in the HU mice, compared with weight-bearing at the late active phase (W-LAP) and HU mice (Fig. 1b). The *Atrogin1* expression level were significantly increased by HU (Supplementary Table 3). The HU-induced up-regulation of *Atrogin1* was attenuated by the intermittent weight-bearing, and this level in W-EAP mice was significantly lower than that in W-LAP mice (Supplementary Table 3). *Murf1* at 1st ZT21 expression level was significantly decreased by W-EAP compared with CON and HU (Fig. 1c). Clock genes expressions serum corticosterone level, and the phosphorylation level of p70S6K, S6 and Akt were not changed between W-EAP and W-LAP mice, except for a significantly decreasing of *Rorα* at 1st ZT21 in W-EAP mice (Fig. 1d–m and Supplementary Table 3). Chronic HU for 14 days significantly decreased the gastrocnemius muscle weight, and the W-EAP attenuated the HU-induced muscle atrophy and body weight loss (Fig. 4a–c). The gastrocnemius muscle weight of W-EAP mice was higher than that of W-LAP mice (Fig. 4a). Food intake was not different among all groups (Fig. 4d). The hourly locomotor activity level during active phase was decreased in HU, W-EAP and W-LAP mice (Fig. 4f), and W-EAP increase the locomotor activity during late active phase (no significant difference). The total activity levels were not changed significantly however seemed to decrease in HU, W-EAP and W-LAP mice (Fig. 4g). The activity level during the respective weight-bearing times were not different between the W-EAP and W-LAP mice (Fig. 4h).

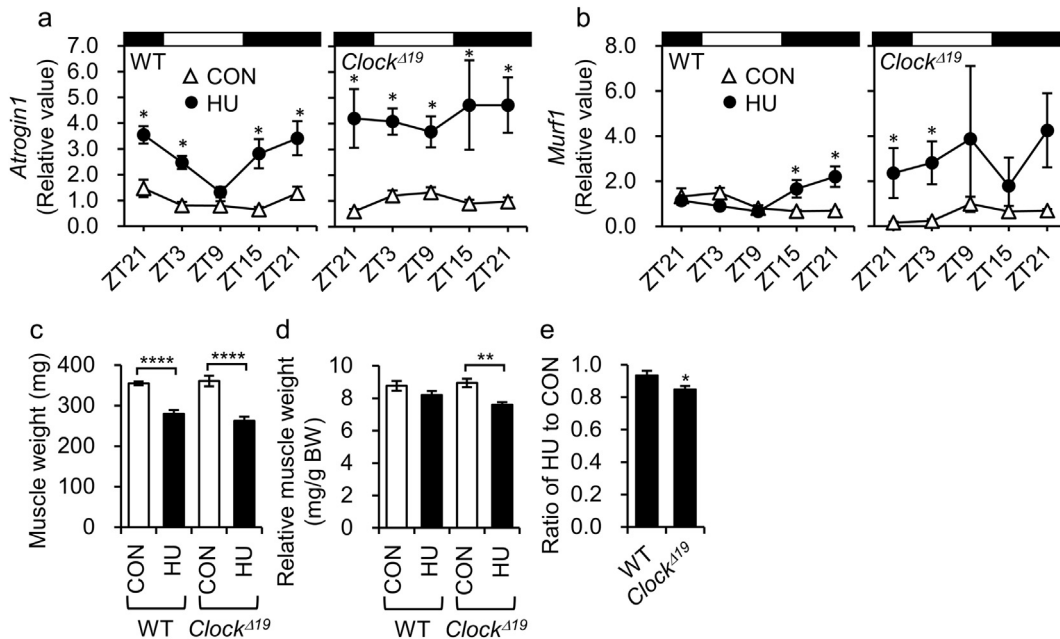


Fig. 2. Day-night variations of *Atrogin1* and *Murf1* expressions in gastrocnemius muscle and muscle weight of control (CON) and hindlimb-unloaded (HU) wild-type (WT) and *Clock* mutant (*Clock*^{Δ19}) mice. The expression levels of (a) *Atrogin1* and (b) *Murf1* were examined by real-time RT-PCR. Data are expressed as the mean ± standard error (n = 4–5 at each time point) and normalized by the CON group of each genotype. *P < .05 by Kruskal-Wallis test with a two-stage linear step-up procedure of Benjamini, Krieger and Yekutieli test. Clock genes expression were shown in Supplementary Fig. 9. (c) Gastrocnemius muscle weight and (d) relative gastrocnemius muscle weight of CON (white) and 14 days HU (black) in WT and *Clock*^{Δ19} mice. (e) Ratio of relative muscle weight in the HU group to that in the CON group of each genotype. Data are expressed as the mean ± standard error (n = 6). *P < .05, **P < .01, ****P < .0001 by unpaired t-test or two-way analysis of variance (ANOVA) with a Sidak post hoc test.

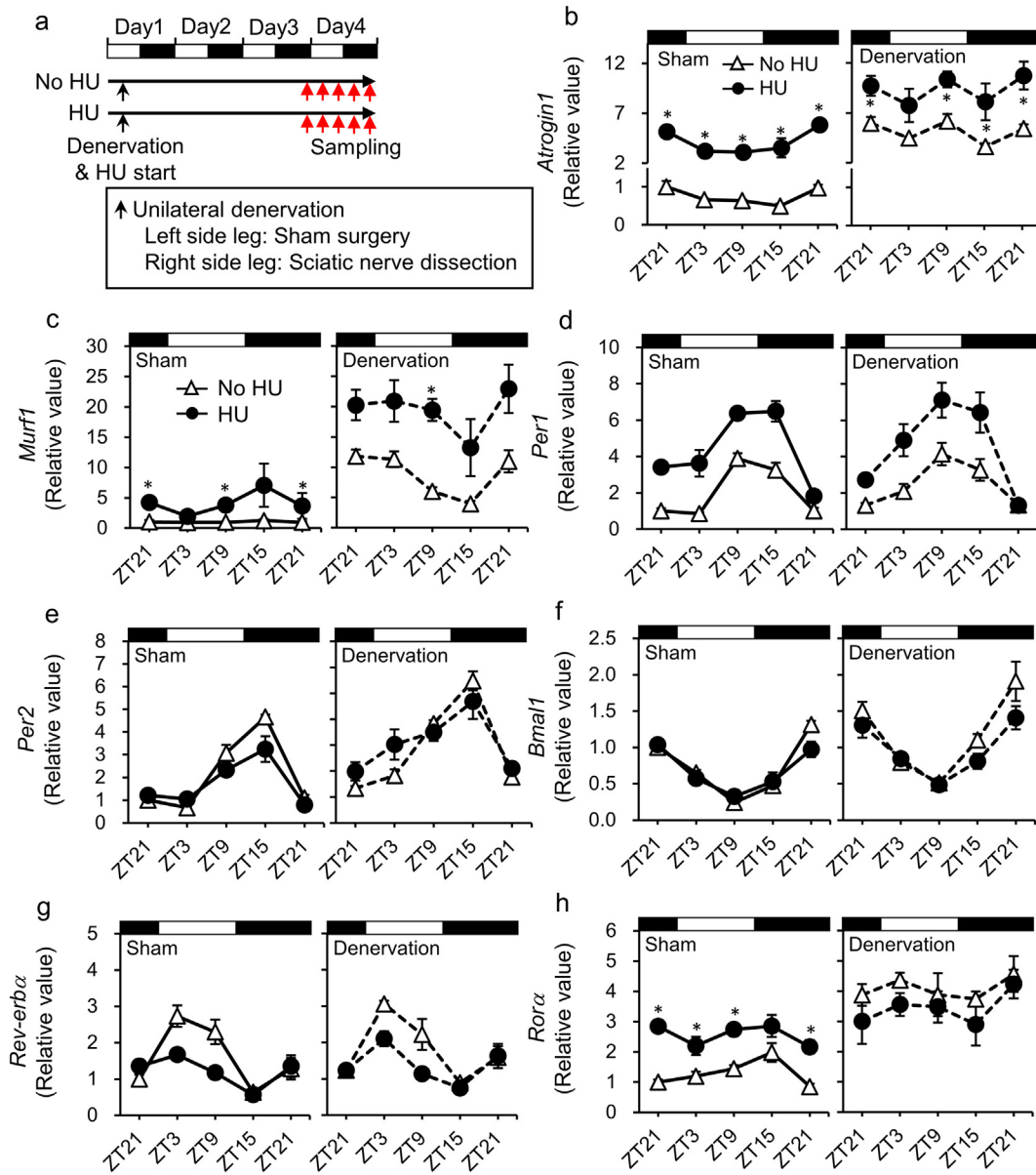


Fig. 3. Effect of sciatic nerve dissection on *Atrogin1* and *Murf1* and clock genes expression in hindlimb unloaded mice. (a) The experimental scheme of denervation and hindlimb unloading (HU). Mice were subjected to unilateral denervation of the sciatic nerve on day 1. After unilateral denervation, HU was started for 4 days. The muscles were collected every 6 h from ZT21 on day 3 to ZT21 on day 4, as indicated by the red arrows. (b) *Atrogin1*, (c) *Murf1*, (d) *Per1*, (e) *Per2*, (f) *Bmal1*, (g) *Rev-erba*, (h) *Rora* expression in the gastrocnemius muscle of the sham-treated leg (left-side) and denervated leg (right-side) of No HU (white) and HU (black). Data are expressed as the mean \pm standard error ($n = 4-5$ at each time point). * $P < .05$ by Kruskal-Wallis test with a two-stage linear step-up procedure of Benjamini, Krieger and Yekutieli test.

In WT mice, HU-induced *Atrogin1* up-regulation at ZT21 was not observed in the W-EAP mice while its increasing was remained in W-LAP mice (Fig. 5a left). On the other hand, weight-bearing at early and late active phase did not prevent HU-induced *Atrogin1* expression in *Clock* ^{Δ 19} mice (Fig. 5a right). *Murf1* expression were remarkably increased by HU and the preventive timing-dependent effect of weight-bearing was not observed in *Clock* ^{Δ 19} mice (Fig. 5b). In addition, the preventive effects of W-EAP in WT mice on the muscle atrophic phenotype, including the gastrocnemius muscle weight and muscle fiber CSA, were not observed in *Clock* ^{Δ 19} mice (Fig. 5c–f). The pattern of locomotor activity in *Clock* ^{Δ 19} mutant mice was changed by the timing of weight-bearing, and the locomotor activity of *Clock* ^{Δ 19} mutant mice was increased during weight-bearing in each group. However, the total amount of locomotor activity was not changed (Supplementary Fig. 6).

4. Discussion

In this study, we showed that (i) *Atrogin1* expression showed day-night variation in gastrocnemius muscles under the HU-induced atrophic condition, (ii) their day-night variations were regulated by a circadian clock, and (iii) the preventive effects of intermittent weight-bearing on the HU-induced muscle atrophy depended on its timing.

The rhythmic expression of *Atrogin1* was observed in a normal skeletal muscle from microarray data reported previously [10,12]. The *Atrogin1* expressions showed day-night variation under the HU condition, and their day-night variation was not observed in *Clock* ^{Δ 19} mice. To elucidate the mechanism of rhythmic *Atrogin1* expression, we first expected three factors to regulate their expression levels: feeding-cycle, an intrinsic muscle clock and a glucocorticoid effect. *Atrogin1*

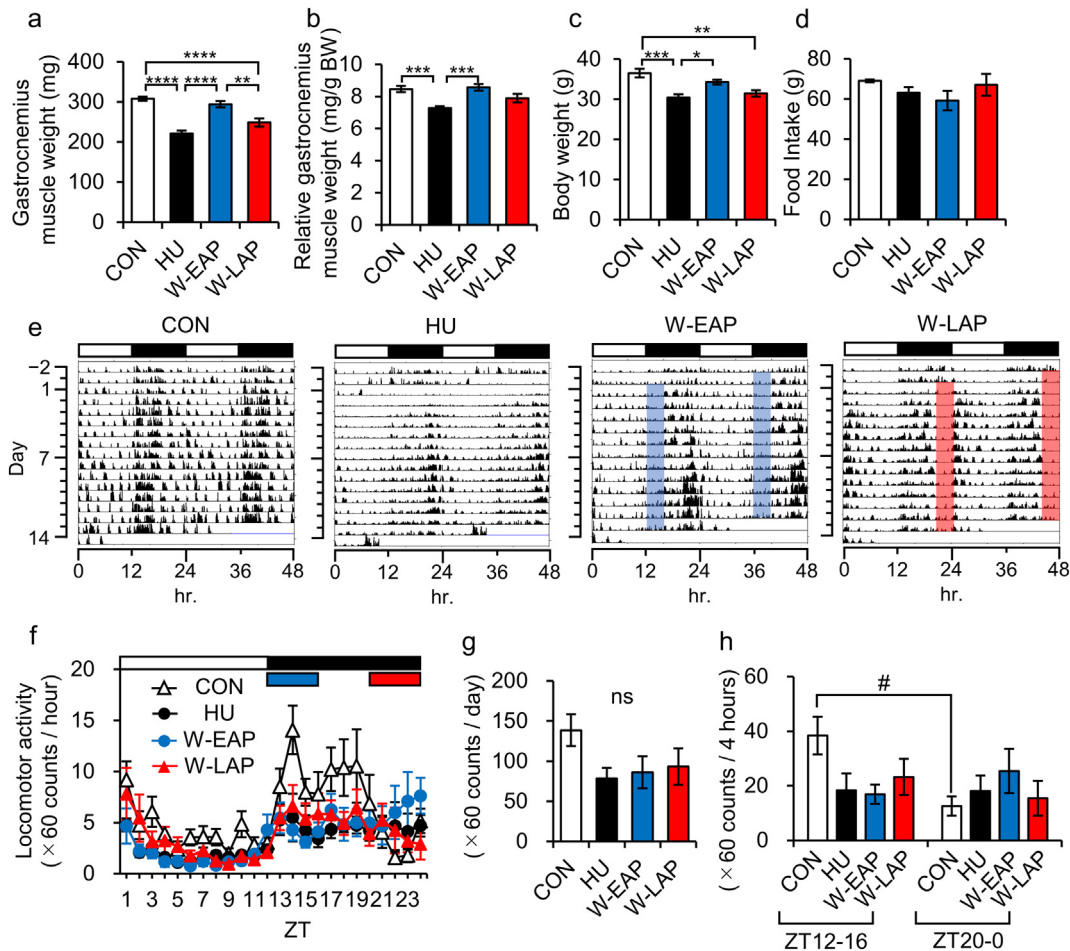


Fig. 4. Timing-dependent effects of weight-bearing on hindlimb-unloading (HU)-induced muscle atrophy. (a) Gastrocnemius muscle weight, (b) relative gastrocnemius muscle weight, (c) body weight, and (d) food intake of Control (CON), HU, and weight-bearing during early active phase (W-EAP) and late active phase (W-LAP) mice. (e) Representative double-plotted actograms of locomotor activity determined by an infrared sensor in CON, HU, W-EAP and W-LAP mice. The blue or red shadow indicates the weight-bearing period. (f) Wave forms of locomotor activity analyzed during experimental periods. (g) Daily total locomotor activity and (h) activity during early (ZT12–16) and late (ZT20–24) active phase of CON, HU, W-EAP and W-LAP mice. Data are expressed as the mean \pm standard error (a, b, c; n = 6–9, d; n = 4–6, f, g, h; n = 4–6). * P < .05, ** P < .01, *** P < .001, **** P < .0001 by analysis of variance (ANOVA) with a Tukey post hoc test. # P < .05 by Kruskal-Wallis test with a two-stage linear step-up procedure of Benjamini, Krieger and Yekutieli test.

expression is regulated by nutritional signaling via the Akt-FOXO pathway [36] or glucocorticoid receptor signaling [37]. Additionally, several *E-box* binding sites exist in the promoter region of *Atrogin1* gene. These reports suggest that feeding time, glucocorticoid rhythm, or the intrinsic muscle clock drive the day-night expression of *Atrogin1*.

No changes were observed in the *Atrogin1* expression level and its phase between NRF and DRF mice, suggesting that feeding timing did not involve in its day-night expression. However, the phase of *Atrogin1* and *Murf1* in NRF and DRF mice was shifted compared with that in the mice under the free feeding condition (Fig. 1 and Supplementary Fig. 5). Although timing of feeding is suggested not to be involved in its day-night expression, time-restricted feeding may partially affect the phase of *Atrogin1* and *Murf1*, compared with the free feeding condition. It is likely to relate on the fasting periods because fasting regulates *Atrogin1* and *Murf1* expression [15]. In addition, compared with NRF, DRF changed the phase of muscle clock genes to an antiphase oscillation. Furthermore, the day-night fluctuation of *Atrogin1* in sham muscle from HU mice was not observed in denervated muscle from HU mice, although most of the clock genes were oscillated in the denervated muscle from HU mice. This suggests that the effects of intrinsic muscle clock on the regulation of *Atrogin1* fluctuation could be small. To be clear on the role of intrinsic muscle clock on the day-night variation of *Atrogin1*, further studies using tissue-specific clock gene deletion mice are necessary.

In this study, serum corticosterone level in HU mice tended to be higher and exhibited a circadian rhythm (Fig. 1i), and its phase tended to be advanced by DRF compared with NRF (Supplementary Fig. 5i). It is well-known that the phase of corticosterone is affected by time-restricted feeding [38,39]. Considering that the DRF did not change the expression of *Atrogin1* and *Murf1* regardless of the phase shift of corticosterone by time-restricted feeding, this suggests that serum corticosterone rhythm does not affect their day-night expression under the HU condition.

It is thought that oscillation of global circadian genes expression in skeletal muscle is driven not only by a muscle clock but additionally by a neuronal external cue such as physical activity rhythm [10]. In the present study, denervated muscle did not show the normal day-night expression cycle of *Atrogin1* under the HU condition, while their day-night variations were observed in the sham-surgery contralateral muscles from the same animals. Denervation influences clock gene expression [10,27]. In the present study, denervation increased *Per2*, *Bmal1*, and *Rora* expression and abolished the rhythmicity of *Rora*. The rhythmicity and phase of clock genes expression except for *Rora* remained in the denervated muscles, suggesting that the involvement of these clock genes in day-night *Atrogin1* expression could be small. In addition, considering that the ablation of *Rora* rhythmic expression was observed in the sham muscle of HU mice, although the expression of *Atrogin1* oscillated in this muscle, *Rora* was less likely to regulate

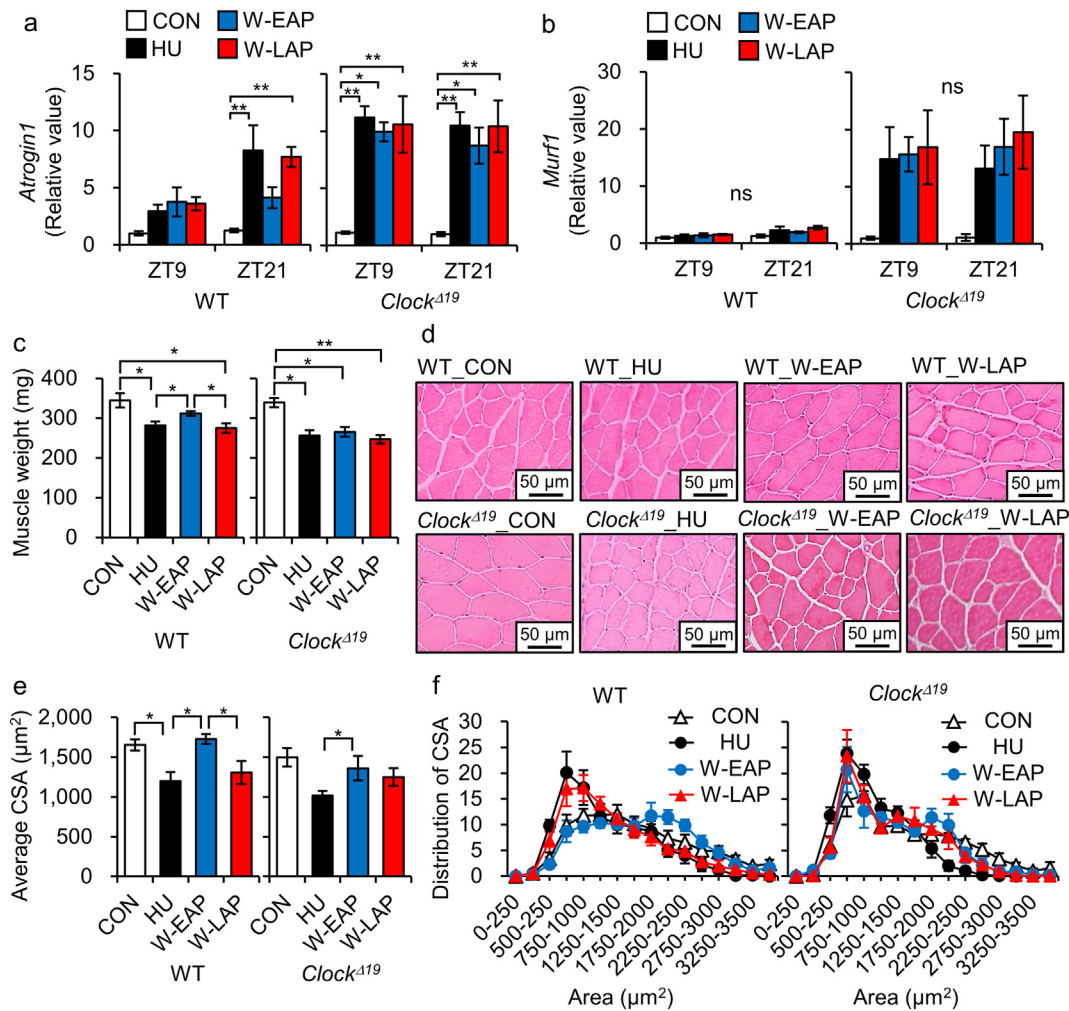


Fig. 5. Role of circadian rhythm on timing-dependent preventive effects of weight-bearing on *Atrogin1* and *Murf1* expression and muscle atrophy. (a) *Atrogin1* and (b) *Murf1* expression at ZT9 and ZT21 in gastrocnemius muscle of wild-type (WT) and *Clock* mutant (*Clock*^{Δ19}) mice. Once per day, weight-bearing was conducted at the early (W-EAP) or late (W-LAP) active phase. (c) Gastrocnemius muscle weight from control (CON), hindlimb-unloading (HU), W-EAP and W-LAP groups in WT and *Clock*^{Δ19} mice. (d) Representative H&E stain from the all groups in WT and *Clock*^{Δ19} mice. Scale bar, 50 μ m. (e) Average size of the cross-sectional areas (CSAs) of muscle fibers from WT and *Clock*^{Δ19} mice. (f) The distributions of the CSAs of muscle fibers in WT and *Clock*^{Δ19} mice plotted as frequency histograms. Data are expressed as the mean \pm standard error, (a, b; n = 4–8 at each time point, c; n = 5–9, e, f; n = 4–6). **P* < .05, ***P* < .01 by Kruskal-Wallis test with a two-stage linear step-up procedure of Benjamini, Krieger and Yekutieli test.

the day-night expression of *Atrogin1*. This result suggests that a circadian neuronal cue or locomotor activity controls the HU-induced *Atrogin1* rhythmic expression independent of muscle clocks. Nakao et al. reported that *Atrogin1* did not show a rhythmic expression in denervated muscles [27], in agreement with our results. The dissection of the sciatic nerve remarkably inhibits muscle activity, and Dyer et al. reported that physical activity regulated the rhythm of circadian gene expression via a muscle contraction-related Ca²⁺-dependent pathway in muscles [10], suggesting that circadian locomotor activity rhythms drove circadian genes expression. Circadian regulation of motor neuron activity could be important for the day-night variation of *Atrogin1* expression. Additionally, the sciatic nerve includes not only a motor nerve but an autonomic nerve as well [40]. Further studies are warranted to determine the role of a clock via a motor or autonomic neuronal signal on the oscillation of *Atrogin1* genes expression.

The day-night expression of *Atrogin1* and *Murf1* was not observed in the soleus muscle (Supplementary Fig. 3. The preventive effect of W-EAP was likewise not observed in the soleus muscle (Supplementary Figs. 3 and 7). These results suggest that the effect of circadian rhythm on skeletal muscle function depends on the muscle fiber type. It is generally thought that skeletal muscle fibers are classified into two main types: slow-twitch (type1) muscle fibers and fast-twitch (type2A, type2X, and type2B) muscle fibers. Gastrocnemius muscles are

predominantly made up of fast-type fibers, while soleus muscles mainly include slow-twitch fibers. It has been reported that the responses of gene expression such as that of *Atrogin1* and *Murf1* and muscle atrophy were different between fast-type muscles and slow-type muscles [41,42]. Several rhythmic genes were differentially expressed between fast- and slow-type muscles [10]. Therefore, it is possible that the circadian regulation of *Atrogin1* and timing-dependent effects of weight-bearing could depend on the muscle fiber types [42].

The circadian clock-controlled *Atrogin1* and *Murf1* expression could be important for the maintenance of muscle mass in the HU condition. In our study, the *Clock*^{Δ19} mice showed higher response of *Atrogin1* and *Murf1* to the HU condition and the HU-induced decreasing ratio of muscle weight to the control muscle was higher in *Clock*^{Δ19} mice. It suggests that *Clock*^{Δ19} mice are susceptible to the HU. *Bmal1* knockout mice show extreme muscle loss with aging [18], though skeletal muscle-specific *Bmal1* knockout mice did not show this phenotype [11], suggesting that a non-muscle clock could control muscle mass. Thus, in our study, the susceptibility to the HU in *Clock*^{Δ19} mice could be caused by a dysfunction of non-muscle clock. The effects of clock disturbance on HU-induced muscle loss were examined using constant light exposure model, considered the main model of central clock disruption. (Supplementary Fig. 8). The constant light exposure did not affect muscle loss, suggesting that central clock disruption is not involved in HU-

induced muscle atrophy. On the other hand, this might be due to the fluctuation of *Atrogin1* expression was maintained under longer periods (>24 h) and did not disrupt its time variation because the constant light schedule in this experiment increased the periods of locomotor activity rhythm, however did not show the arrhythmic pattern. Thus, further studies are required using other clock disturbance models such as a constant high intensity light condition and a ultradian (T7) light cycle schedule.

Preventive effects of an intermittent weight-bearing on muscle loss have been known for a long time. An intermittent weight-bearing regimen for 1 to 4 h per day ameliorates HU-induced soleus muscle atrophy and increase of *Atrogin1* and *Murf1* expression [28,29,43,44]. Consistent with these previous reports, our study showed that intermittent weight-bearing prevented HU-induced gastrocnemius and soleus muscle loss (Fig. 4 and Supplementary Fig. 7). In addition, the present study shows that the timing of weight-bearing in a day is important to prevent from HU-induced muscle atrophy and that a circadian clock may be involved in its timing-dependent effect. The amount of physical activity is one of most important factors to maintain muscle mass [45]. In our study, W-EAP showed a greater preventive effect on gastrocnemius muscle atrophy compared with W-LAP, while the locomotor activity level during weight-bearing was not changed (Fig. 4). This suggests that the preventive effect of W-EAP is independent of the locomotor activity level. Although the amount of activity was not changed by the timing of weight-bearing, W-LAP has slightly increased locomotor activity during early inactive phase (Fig. 4). It is suggested that W-LAP may occur during sleep disturbance. *Atrogin1* expression at ZT21 was suppressed by W-EAP. Considering that *Atrogin1* expression was higher at ZT21 and lower at ZT9, this supposed that W-EAP suppressed a rise of *Atrogin1* and *Murf1* expression in the late active phase. While W-LAP partially suppressed an increase in *Atrogin1* expression compared with HU in a day, it did not decrease completely at ZT21 compared with W-EAP. *Atrogin1* is key molecules for progression of disused muscle atrophy and it is thought that the down-regulation of *Atrogin1* expression attenuates muscle atrophy [23]. Therefore, the greater preventive effect of W-EAP on muscle atrophy could be caused by the down-regulation of *Atrogin1* expression. Interestingly, the muscle of W-EAP mice showed the loss of the *Atrogin1* oscillation. The amplitude of *Rev-erb α* and *Rora*, tended to be decreased in W-EAP mice (Supplementary Table 4). *Rev-erb α* KO mice exhibit muscle loss and the up-regulation of *Atrogin1* and *Murf1* [22]. Thus, the loss of *Atrogin1* oscillation might be due to the down-regulation of *Rev-erb α* rhythmicity by W-EAP.

An intermittent weight-bearing regimen additionally attenuates the down-regulation of mTOR signaling, which is one of the key anabolic processes [29]. In our study, while the phosphorylation of p70S6K was not changed, phosphorylation of S6 and Akt was partially rescued by weight-bearing, but no change was observed by timing of weight-bearing. It indicates that the timing of weight-bearing does not affect muscle anabolic processes. *Myod* was transiently increased in W-EAP mice at the 1st ZT21, but not at the 2nd ZT21 (Supplementary Fig. 2a), suggesting that W-EAP could transiently promote muscle differentiation.

The preventive effect of W-EAP on the muscle loss was not observed in *Clock^{Δ19}* mice (Fig. 5). This suggests that W-EAP attenuates the HU-induced muscle loss by direct regulation via *Atrogin1* or indirect regulation via clock genes. Considering that a circadian signal drives the day-night expression of *Atrogin1*, the preventive effect of W-EAP may be mediated by a neuronal signal. However, further studies are necessary to examine the detailed role of circadian clock genes and the signaling pathways responsible for the preventive effects of W-EAP.

In the present study, we showed that the muscle-specific catabolic factors *Atrogin1* exhibited day-night oscillations in the HU condition. In addition, the preventive effects of weight-bearing are dependent on its timing via a circadian clock and W-EAP was more effective for the attenuation of muscle loss. This study provides the evidence to show the importance of timing for a preventive or therapeutic intervention of exercise and rehabilitation against muscle loss.

Acknowledgments

We thank Dr. Tahara. Yu for his advice on this research.

Funding sources

This work was partially supported by the Council for Science, Technology, and Innovation, SIP, “Technologies for creating next-generation agriculture, forestry, and fisheries” (funding agency: Bio-oriented Technology Research Advancement Institution, NARO) (S.S.) and Japan Society for the Promotion of Science (JSPS) KAKENHI Grant Number 17K18176 (S.A.).

Declaration of interests

The authors declare that no competing interests exist.

Author contributions

S.A. and S.S. planned experiments; S.A., S.K., K.S., R.I., M.T., T.S., N.A., K.T., R.H., A.H., and M.T. performed experiments and analyzed data; S.A., Y.H., K.S. and S.S. contributed to design the automated time-controlled intermittent weight-bearing device; S.A. and S.S. wrote the manuscript.

Appendix A. Supplementary data

Supplementary data to this article can be found online at <https://doi.org/10.1016/j.ebiom.2018.10.057>.

References

- [1] Bass J, Takahashi JS. Circadian integration of metabolism and energetics. *Science* 2010;330(6009):1349–54.
- [2] Balsalobre A, Brown SA, Marcacci L, et al. Resetting of circadian time in peripheral tissues by glucocorticoid signaling. *Science* 2000;289(5488):2344–7.
- [3] Albrecht U. Timing to perfection: the biology of central and peripheral circadian clocks. *Neuron* 2012;74(2):246–60.
- [4] Schibler U, Ripperger J, Brown SA. Peripheral circadian oscillators in mammals: time and food. *J Biol Rhythms* 2003;18(3):250–60.
- [5] Shibata S. Neural regulation of the hepatic circadian rhythm. *Anat Rec A Discov Mol Cell Evol Biol* 2004;280(1):901–9.
- [6] Tahara Y, Shibata S. Chronobiology and nutrition. *Neuroscience* 2013;253:78–88.
- [7] Takahashi JS. Molecular components of the circadian clock in mammals. *Diabetes Obes Metab* 2015;17(Suppl. 1):6–11.
- [8] Miller BH, McDearmon EL, Panda S, et al. Circadian and CLOCK-controlled regulation of the mouse transcriptome and cell proliferation. *Proc Natl Acad Sci U S A* 2007;104(9):3342–7.
- [9] Zhang R, Lahens NF, Ballance HI, et al. A circadian gene expression atlas in mammals: implications for biology and medicine. *Proc Natl Acad Sci U S A* 2014;111(45):16219–24.
- [10] Dyar KA, Ciciliot S, Tagliazucchi GM, et al. The calcineurin-NFAT pathway controls activity-dependent circadian gene expression in slow skeletal muscle. *Mol Metab* 2015;4(11):823–33.
- [11] Dyar KA, Ciciliot S, Wright LE, et al. Muscle insulin sensitivity and glucose metabolism are controlled by the intrinsic muscle clock. *Mol Metab* 2014;3(1):29–41.
- [12] McCarthy JJ, Andrews JL, McDearmon EL, et al. Identification of the circadian transcriptome in adult mouse skeletal muscle. *Physiol Genomics* 2007;31(1):86–95.
- [13] van Moorsel D, Hansen J, Havekes B, et al. Demonstration of a day-night rhythm in human skeletal muscle oxidative capacity. *Mol Metab* 2016;5(8):635–45.
- [14] Aoyama S, Shibata S. The role of circadian rhythms in muscular and osseous physiology and their regulation by nutrition and exercise. *Front Neurosci* 2017;11:63.
- [15] Shavlakadze T, Anwari T, Soffe Z, et al. Impact of fasting on the rhythmic expression of myogenic and metabolic factors in skeletal muscle of adult mice. *Am J Physiol Cell Physiol* 2013;305(1):C26–35.
- [16] Andrews JL, Zhang X, McCarthy JJ, et al. CLOCK and BMAL1 regulate MyoD and are necessary for maintenance of skeletal muscle phenotype and function. *Proc Natl Acad Sci U S A* 2010;107(44):19090–5.
- [17] Harfmann BD, Schroder EA, Kacham MT, et al. Muscle-specific loss of Bmal1 leads to disrupted tissue glucose metabolism and systemic glucose homeostasis. *Skelet Muscle* 2016;6:12.
- [18] Kondratov RV, Kondratova AA, Gorbacheva VY, et al. Early aging and age-related pathologies in mice deficient in BMAL1, the core component of the circadian clock. *Genes Dev* 2006;20(14):1868–73.
- [19] Liu J, Zhou B, Yan M, et al. CLOCK and BMAL1 regulate muscle insulin sensitivity via SIRT1 in male mice. *Endocrinology* 2016;157(6):2259–69.

- [20] Schroder EA, Harfmann BD, Zhang X, et al. Intrinsic muscle clock is necessary for musculoskeletal health. *J Physiol* 2015;593(24):5387–404.
- [21] Woldt E, Sebti Y, Solt LA, et al. Rev-erb- α modulates skeletal muscle oxidative capacity by regulating mitochondrial biogenesis and autophagy. *Nat Med* 2013;19(8):1039–46.
- [22] Mayeuf-Louchart A, Thorel Q, Delhaye S, et al. Rev-erb- α regulates atrophy-related genes to control skeletal muscle mass. *Sci Rep* 2017;7(1):14383.
- [23] Bodine SC, Baehr LM. Skeletal muscle atrophy and the E3 ubiquitin ligases MuRF1 and MAFbx/atrogen-1. *Am J Physiol Endocrinol Metab* 2014;307(6):E469–84.
- [24] Mitch WE, Goldberg AL. Mechanisms of muscle wasting. The role of the ubiquitin-proteasome pathway. *N Engl J Med* 1996;335(25):1897–905.
- [25] Bodine SC, Latres E, Baumhueter S, et al. Identification of ubiquitin ligases required for skeletal muscle atrophy. *Science* 2001;294(5547):1704–8.
- [26] Gomes MD, Lecker SH, Jagoe RT, et al. Atrogen-1, a muscle-specific F-box protein highly expressed during muscle atrophy. *Proc Natl Acad Sci U S A* 2001;98(25):14440–5.
- [27] Nakao R, Yamamoto S, Horikawa K, et al. Atypical expression of circadian clock genes in denervated mouse skeletal muscle. *Chronobiol Int* 2015;32(4):486–96.
- [28] D'Aunno DS, Robinson RR, Smith GS, et al. Intermittent acceleration as a countermeasure to soleus muscle atrophy. *J Appl Physiol* 1985(2):428–33 1992. 72.
- [29] Miyazaki M, Noguchi M, Takemasa T. Intermittent reloading attenuates muscle atrophy through modulating Akt/mTOR pathway. *Med Sci Sports Exerc* 2008;40(5):848–55.
- [30] Kamagata M, Ikeda Y, Sasaki H, et al. Potent synchronization of peripheral circadian clocks by glucocorticoid injections in PER2::LUC-Clock/Clock mice. *Chronobiol Int* 2017;34(8):1067–82.
- [31] Morey-Holton ER, Globus RK. Hindlimb unloading rodent model: technical aspects. *J Appl Physiol* (1985) 2002;92(4):1367–77.
- [32] Aoyama S, Jia H, Nakazawa K, et al. Dietary genistein prevents denervation-induced muscle atrophy in male rodents via effects on estrogen receptor- α . *J Nutr* 2016;146(6):1147–54.
- [33] Yoshida D, Aoki N, Tanaka M, et al. The circadian clock controls fluctuations of colonic cell proliferation during the light/dark cycle via feeding behavior in mice. *Chronobiol Int* 2015;32(8):1145–55.
- [34] Miyazaki M, Schroder E, Edelmann SE, et al. Age-associated disruption of molecular clock expression in skeletal muscle of the spontaneously hypertensive rat. *PLoS One* 2011;6(11):e27168.
- [35] Hughes ME, Hogenesch JB, Kornacker K. JTK_CYCLE: an efficient nonparametric algorithm for detecting rhythmic components in genome-scale data sets. *J Biol Rhythms* 2010;25(5):372–80.
- [36] Sandri M, Sandri C, Gilbert A, et al. Foxo transcription factors induce the atrophy-related ubiquitin ligase atrogen-1 and cause skeletal muscle atrophy. *Cell* 2004;117(3):399–412.
- [37] Shimizu N, Yoshikawa N, Ito N, et al. Crosstalk between glucocorticoid receptor and nutritional sensor mTOR in skeletal muscle. *Cell Metab* 2011;13(2):170–82.
- [38] Challet E, Pevet P, Vivien-Roels B, et al. Phase-advanced daily rhythms of melatonin, body temperature, and locomotor activity in food-restricted rats fed during daytime. *J Biol Rhythms* 1997;12(1):65–79.
- [39] Mukherji A, Kobiita A, Chambon P. Shifting the feeding of mice to the rest phase creates metabolic alterations, which, on their own, shift the peripheral circadian clocks by 12 hours. *Proc Natl Acad Sci U S A* 2015;112(48):E6683–90.
- [40] Minokoshi Y, Kim YB, Peroni OD, et al. Leptin stimulates fatty-acid oxidation by activating AMP-activated protein kinase. *Nature* 2002;415(6869):339–43.
- [41] Macpherson PC, Wang X, Goldman D. Myogenin regulates denervation-dependent muscle atrophy in mouse soleus muscle. *J Cell Biochem* 2011;112(8):2149–59.
- [42] Wiberg R, Jonsson S, Novikova LN, et al. Investigation of the Expression of Myogenic Transcription Factors, microRNAs and Muscle-specific E3 Ubiquitin Ligases in the Medial Gastrocnemius and Soleus Muscles following Peripheral Nerve Injury. *PLoS One* 2015;10(12):e0142699.
- [43] Thomason DB, Herrick RE, Baldwin KM. Activity influences on soleus muscle myosin during rodent hindlimb suspension. *J Appl Physiol* (1985) 1987;63(1):138–44.
- [44] Bangart JJ, Widrick JJ, Fitts RH. Effect of intermittent weight bearing on soleus fiber force-velocity-power and force-pCa relationships. *J Appl Physiol* (1985) 1997;82(6):1905–10.
- [45] Thompson LV. Skeletal muscle adaptations with age, inactivity, and therapeutic exercise. *J Orthop Sports Phys Ther* 2002;32(2):44–57.